The American Journal of Human Genetics, Volume *104*

Supplemental Data

Recurrent Germline *DLST* Mutations in Individuals with Multiple Pheochromocytomas and Paragangliomas

Laura Remacha, David Pirman, Christopher E. Mahoney, Javier Coloma, Bruna Calsina, Maria Currás-Freixes, Rocío Letón, Rafael Torres-Pérez, Susan Richter, Guillermo Pita, Belén Herráez, Giovanni Cianchetta, Emiliano Honrado, Lorena Maestre, Miguel Urioste, Javier Aller, Óscar García-Uriarte, María Ángeles Gálvez, Raúl M. Luque, Marcos Lahera, Cristina Moreno-Rengel, Graeme Eisenhofer, Cristina Montero-Conde, Cristina Rodríguez-Antona, Óscar Llorca, Gromoslaw A. Smolen, Mercedes Robledo, and Alberto Cascón

Figure S1

A

neutral deleterious % expected accuracy

Mutation	PredictSNP	MAPP	PhD-SNP	PolyPhen-1	PolyPhen-2	SIFT	SNAP
p.Arg231Asn	**87%**	72%	59%	74%	81%	79%	81%
p.Asp304Asn	**75%**	78%	68%	67%	41%	90%	77%
p.Gly374Glu	**87%**	91%	68%	74%	81%	79%	89%
p.Tyr422Cys	**72%**	74%	61%	74%	81%	79%	89%

B

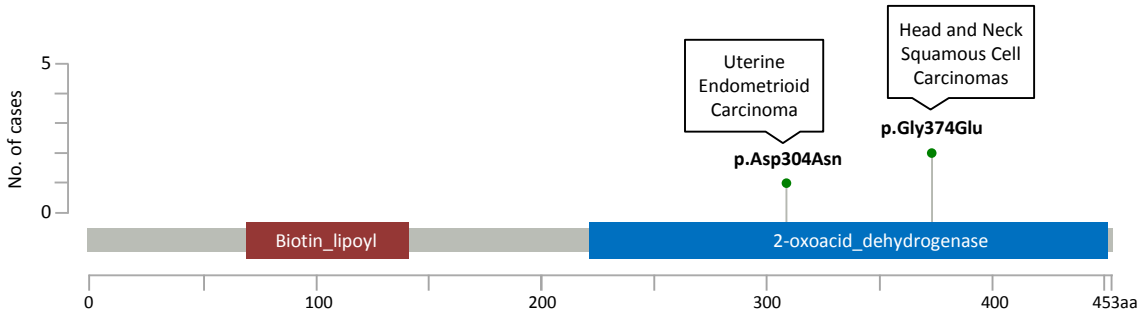

Figure S1. (A) Prediction of the effects of the different DLST substitutions by seven consensus classifiers using PredictSNP. **(B)** Previously reported DLST variants found in endometrioid carcinoma (p.Asp304Asn) and upper aerodigestive tract squamous cell carcinoma (p.Gly374Glu). Data are from cBioPortal. The number of cases of each variant is represented by vertical bars.

Figure S2

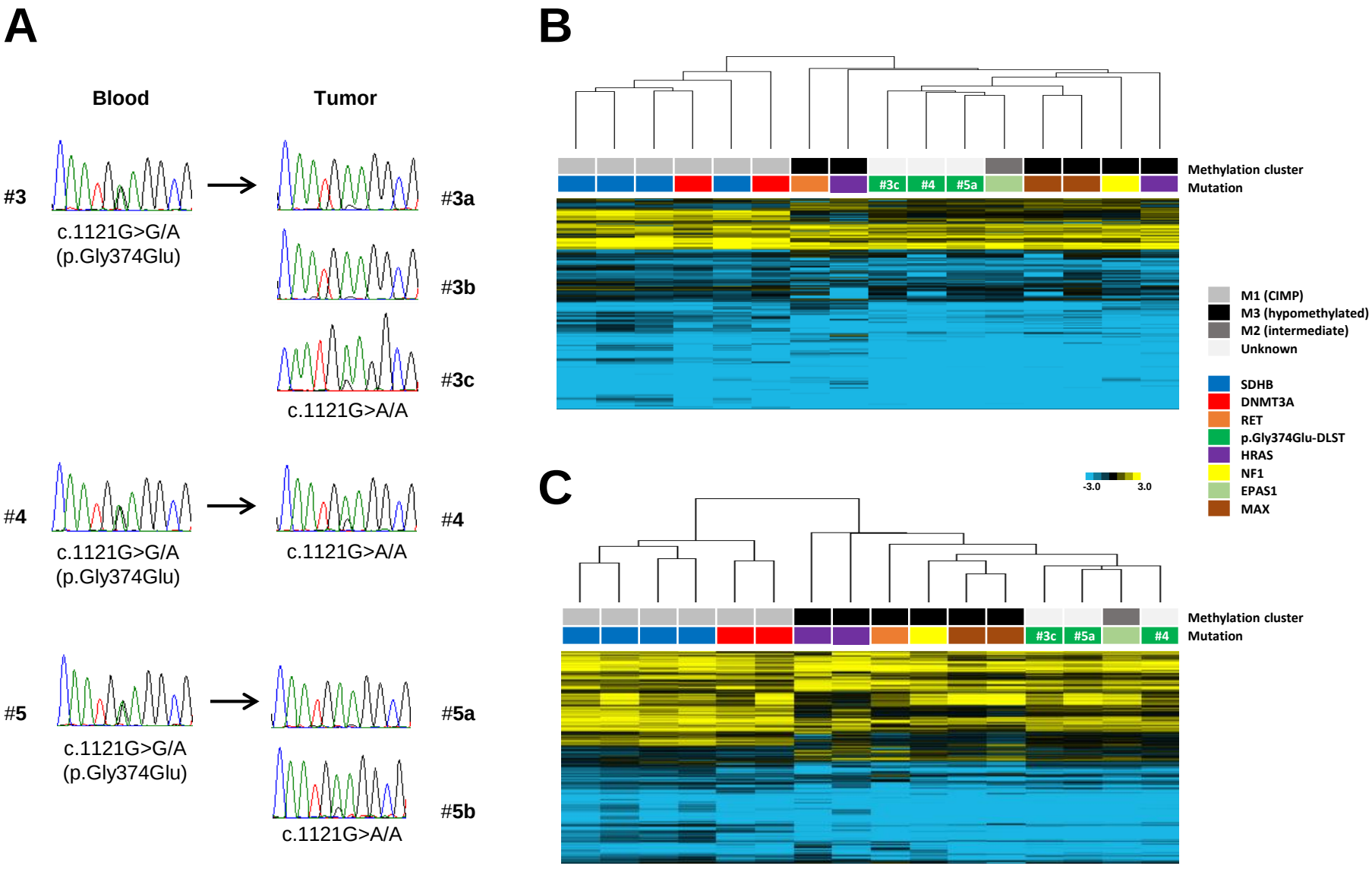

Figure S2. (A) Sanger sequencing of six tumors from three unrelated individuals (p.Gly374Glu) showing LOH of the wild-type *DLST* allele. **(B)** Hierarchical clustering of methylation data from p.Gly374Glu-DLST tumors (n=3; #3c, #4, #5a) compared to controls (n=13; 2 *DNMT3A,* 4 *SDHB,* 1 *EPAS1,* 2 *MAX, 2 HRAS,* 1 *RET* and 1 *NF1*-mutated tumors). Tumors (denoted with different colors depending on the gene mutated) were split up between different methylation clusters of PPGLs[30]: cluster M1 (denoted in light grey) which included SDHB- (n=4) and *DNMT3A*- (n=2) mutated tumors, cluster M2 (denoted in dark grey) which included one *EPAS1*-mutated tumor, and cluster M3 (denoted in black) which included *RET*- (n=1), *HRAS*- (n=2), *NF1*- (n=1), and *MAX*- (n=2) mutated PPGLs. City Block (SD=1.4) and complete linkage characteristics were used for the analysis. **(C)** Hierarchical clustering of the 16 mutated tumors from panel (B) based on methylation data for 125,112 probes corresponding to 4,662 genes with CpG sites reported as significantly hypermethylated in M1 (SDHx-mutated) PPGLs. The three tumors carrying the p.Gly374Glu-DLST variant (#3c, #4 and #5a), were clustered together and separated from cluster M1 samples. Uncentered correlation (SD=1.5) and complete linkage characteristics were used for the analysis.

Figure S3

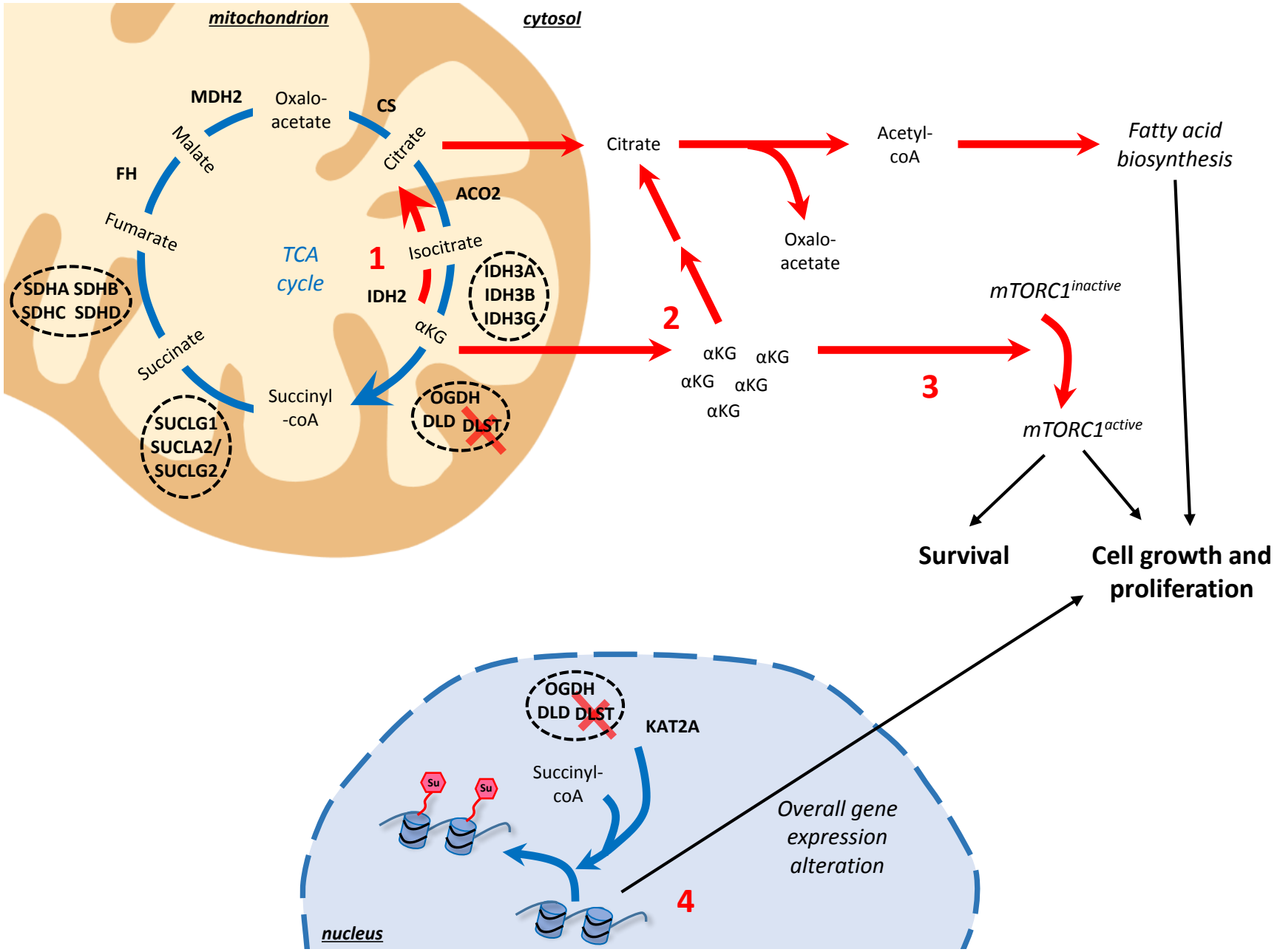

Figure S3. Schematic representation of theoretical extra-mitochondrial consequences due to αKG accumulation upon inactivation of OGDH-complex DLST subunit (denoted by a red cross). 1) Loss of activity of the OGDH complex and the unbalance of the αKG/citrate ratio can lead to a TCA cycle functioning in a reverse mode, ultimately supporting *de novo* fatty acid synthesis and favoring tumor growth. 2) In addition, perturbations of the αKG pool affect the cytoplasmic level of acetyl-CoA by its conversion to citrate, increasing fatty acid biosynthesis. 3) High cytosolic levels of αKG may also promote aberrant mammalian target of rapamycin complex 1 (mTORC1) activation, which might be beneficial for cancer cells by promoting survival and proliferation. 4) Finally, the OGDH complex, associated with KAT2A in gene promoter regions, plays an instrumental role in the regulation of gene expression by histone succinylation. Therefore, loss of OGDH activity by *DLST* mutation may lead to altered overall gene expression and tumor cell proliferation. Blue arrows denote the cellular processes in which the wild-type OGDH complex is involved, and red arrows indicate alternative pathways activated upon loss of OGDH activity.

Figure S4

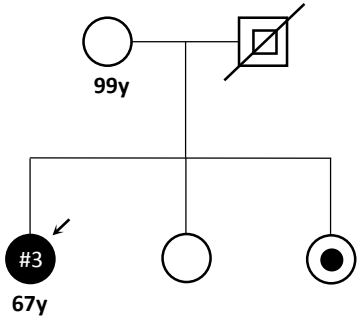

#3 PGL para-aortic (27y) + PGL renal and PGL pelvic (35y) + PGL pre-sacrum (41y) + PGL Zuckerkandl (49y) + PGL para-aortic and PGL iliac (53y, operated with 66y) + uterine endometrioid carcinoma (66y) - p.Gly374Glu

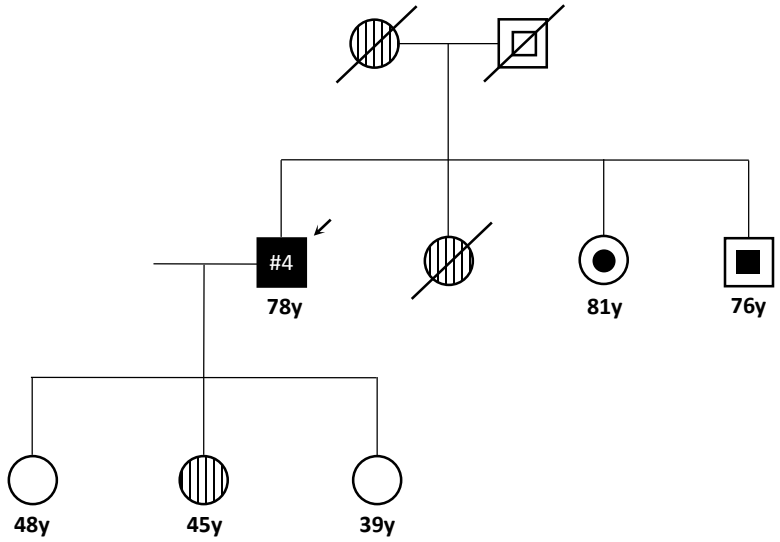

#4 PGL para-adrenal (38y) + PGL para-aortic (62y) + PGL para-vertebral (69y) - p.Gly374Glu

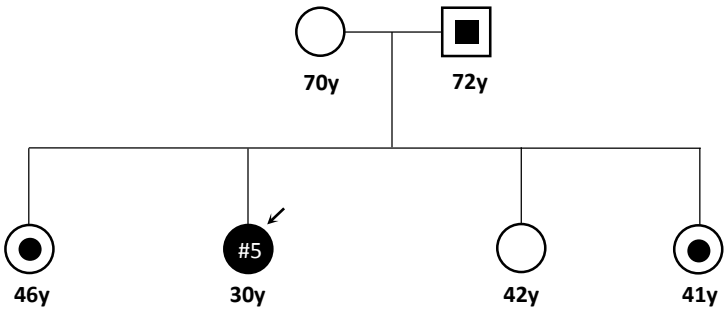

#5 PGL para-adrenal + PGL retroperitoneal (24y) + PGL para-adrenal *vs* recidivation (29y) - p.Gly374Glu

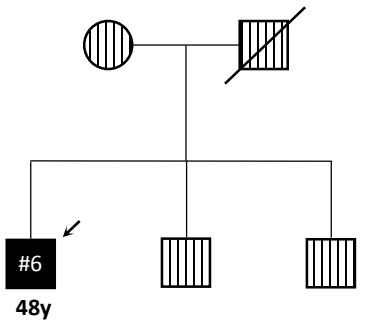

#6 PGL pre-sacrum + two PGLs para-aortic + PGL renal (29y) - p.Gly374Glu

Figure S4. Pedigrees of individuals #3, #4, #5 and #6. The proband of each pedigree is indicated by a black arrowhead; striped symbols indicate individuals in which no genetic test was performed; internal filled symbols indicate asymptomatic (no clinical surveillance performed) individuals carrying the p.Gly374Glu variant; internal empty symbols indicate individuals predicted to carry the p.Gly374Glu variant.

Table S1. Clinical data of the PPGL patients included in the study

Number of cases	*Gender*	*Median age at onset (range)*	*Patients with single (S) or multiple (M) tumors*	*Location of tumors*	*Catecholamine phenotype*	*Metastatic cases*
104	m: **43** f: **59** U: **2**	**49y** (8-82)	S: **77** M: **27**	PCC: **57** TAP: **22** H&N: **14** Misc: **9** U: **2**	NORA: **34** ADR: **17** NF: **14** DOPA: **8**	**11**

m: male; f: female; U: unknown; PCC: pheochromocytoma; TAP: thoracic-abdominal-pelvic paraganglioma; H&N: head and neck paraganglioma; Misc: miscellaneous; NORA: noradrenergic; ADR: adrenergic; NF= non functional, DOPA: dopaminergic

Table S2. Genes included in the targeted next-generation sequencing panel

ACO1
ACO2
CS
DLAT
DLD
DLST
GOT1
GOT2
IDH1
IDH2
IDH3A
IDH3B
IDH3G
MDH1
OGDH
OGDHL
PC
PCK1
PCK2
PDHA1
PDHA2
PDHB
SLC25A1
SLC25A10
SLC25A11
SLC25A13
SUCLA2
SUCLG1
SUCLG2
FH
MDH2
SDHA
SDHB
SDHC
SDHD
SDHAF1
SDHAF2

Table S3. Targeted NGS variants identified

Gene symbol	Description	Nucleotide variant	Chr	Coordinate	Consequence	SIFT	PolyPhen	cDNA variant	Protein variant	GnomAD (carriers:total individuals)
DLST GenBank: NM_001933	Dihydrolipoamide S-Succinyltransferase	G>G/A	14	75361034	Missense variant	deleterious	probably_damaging	c.692G>A	p.Arg231Gln	2:123,099
		G>G/A	14	75366634	Missense variant	tolerated	probably_damaging	c.910G>A	p.Asp304Asn	-
		G>A/A	14	75367830	Missense variant	deleterious	probably_damaging	c.1121G>A	p.Gly374Glu	2:123,121
		A>A/G	14	75368936	Missense variant	deleterious	probably_damaging	c.1265A>G	p.Tyr422Cys	3:137,372
		T>T/A	14	75367766	Splice region variant	-	-	c.1060-3T>A	-	1:122,641
IDH1 GenBank: NM_001282387	Isocitrate Dehydrogenase (NADP(+)) 1, Cytosolic	T>T/A	2	209113206	Missense variant	deleterious	probably_damaging	c.301A>T	p.Asn101Tyr	1:123,132
SLC25A10 GenBank: NM_012140	Solute Carrier Family 25 Member 10	C>C/T	17	79682747	Missense variant	deleterious	probably_damaging	c.353C>T	p.Thr118Met	-
SLC25A11 GenBank: NM_003562	Solute Carrier Family 25 Member 11	C>C/T	17	4841465	Missense variant	deleterious	probably_damaging	c.721G>A	p.Asp241Asn	1:123,042
SUCLG1 GenBank NM_003849	Succinate-CoA Ligase Alpha Subunit	G>G/T	2	84660523	Missense variant	deleterious	probably_damaging	c.626C>A	p.Ala209Glu	4:123,001

Chr: chromosome; SIFT: 'Sorting Intolerant From Tolerant' algorithm prediction; PolyPhen: 'Polymorphism Phenotyping' algorithm prediction; GnomAD: frequency of the variant in the gnomAD database